Light-to-current and current-to-light coupling in plasmonic systems

N. Noginova, A. V. Yakim, J. Soimo, L. Gu, and M. A. Noginov

Phys. Rev. B **84**, 035447 — Published 28 July 2011

DOI: 10.1103/PhysRevB.84.035447

Light-to-Current and Current-to-Light Coupling in Plasmonic Systems

N. Noginova, A. V. Yakim, J. Soimo, L. Gu, M. A. Noginov

Center for Materials Research, Norfolk State University, Norfolk VA 23504

nnoginova@nsu.edu

In thin silver films, we have observed strong photon drag effect (PDE) enhanced by surface plasmon polaritons (SPPs) excited in a Kretschmann geometry at the SPP resonant angle. A weaker PDE of an opposite polarity has been detected at off-resonance incidence angles. We have also found that SPPs can be controlled by an external dc current propagating in the film. Both observed phenomena are mediated by electron-plasmon coupling and can find applications in plasmonic nanocircuitry, combining advantages of compact electronics and fast photonics.

PACS : 73.20.Mf; 73.50.–h

1. Introduction

Plasmonic metamaterials have promise to revolutionize information technology by combining advantages of compact electronics and fast photonics. Coupling of electric and optical effects in plasmonic circuit elements is of imminent importance for photonic nanocircuitry applications [1] as it may provide an opportunity to include plasmonic elements in electronic circuits and/or control surface plasmon effects electrically.

Photon drag effect (PDE) – generation of *dc* electric current or electromotive force under optical illumination – has been first observed in semiconductors in 1970 [2,3]. In first approximation, PDE is commonly discussed in terms of radiation pressure, *i.e.* momentum (or quasi-momentum) transfer from photons to charge carriers. However, the sign and the magnitude of PDE can be different from those solely determined by a direct photon-to-electron momentum

transfer, depending on the energy band structure, electronic transitions, and relaxation processes involved [4-13]. One of the mechanisms of enhanced PDE in semiconductors and metals originates from a combination of directional transition selectivity associated with the Doppler effect and different carriers' mobilities in ground and excited states [8,9].

Photogalvanic effect discussed in [10-12] is associated with diffusive scattering of electrons off the metal surface that can result in the net flow of electrons away from the surface and against the in-plane component of the photon wave-vector. Similar considerations were used in the hydrodynamic model of PDE [14], based on a combination of the Maxwell's equations and the hydrodynamic equations for a jellium surface obliquely illuminated by a monochromatic light. Another mechanism of a PDE is associated with a gradient of light intensity and diffusive current flow resulting from non-uniform distribution of excited state electrons [9].

The photon drag effect in bulk metals has been observed experimentally at low temperatures [10-12]. The detected signal demonstrated strong dependence on light polarization [12], in reasonable agreement with the photogalvanic theory. Plasmon-induced enhancement of PDE was observed in thin gold films [15], where the phenomenon was explained by an increase of light absorption under resonant condition of surface plasmon polariton (SPP) excitation. The recent theoretical study [16] has predicted a much stronger plasmon-induced photon drag effect in thin metallic nanowires, which was not only due to increased optical fields inside nanowires but rather due to extremely high gradients of electric fields (striction forces).

Of imminent relevance to this work are the effects of electron-plasmon coupling known in a variety of systems, such as electron ensembles with long-range Coulomb potential found in semiconductors, superconductors and metals, which can affect both electron transport and optical properties of materials [17-20]. Thus, the energy transfer between individual electrons and

collective modes has been observed in photon echo experiments in GaAs [17]. Plasmon-related change in carriers' mobility [18], enhancement of the Coulomb drag in parallel quantum wells [19], and nonlinearity of voltage-current curves in metal-semiconductor point contacts [20] associated with plasmon excitations have been reported over the years. Another known example of the electron-plasmon coupling is an excitation of SPPs with an electron beam [21].

In this work, in order to better understand the origin of a photon drag effect in metals and its enhancement by surface plasmon polaritons as well as to explore effects determined by coupling of surface plasmons with electronic transport, we have experimentally studied PDE in silver films both under the *resonant* condition of SPP excitation (in Kretschmann geometry) and at the incidence angles at which SPPs were not excited. We have also explored the possibility of controlling SPPs externally by electric currents propagating in metallic films.

2. Experimental Observation of the Photon Drag Effect in a Kretschmann Geometry

Experimentally, 2 mm x 15 mm strips of thin silver films, 30-60 nm, were deposited on high-index glass prisms, n=1.78, using thermal vapor deposition technique. Two electrical contacts were attached to opposite ends of the stripes at the distance of ~12 mm from each other. Electric (dc) resistances of the samples with contacts and wires were in the range of 9-30 Ohm. The experimental setup used in the first series of experiments is shown in Fig. 1 a. A prism with the film was placed on a rotating stage and illuminated from the cathetus side with p polarized laser light (~5 ns pulses of an optical parametric oscillator tunable between 430 and 700 nm). The diameter of the excitation spot, ~2.5 mm, was slightly larger than the width of the strip. When the sample's reflectance was measured as a function of an incidence angle, a characteristic dip manifesting excitation of SPPs [22] has been observed, Fig. 1b. Remarkably, laser light illumination induced an electric signal (measured with 1 GHz oscilloscope, 50 Ω input

impedance), which temporal profile approximately corresponded to that of the laser pulse, Fig 1c.

The electric signal – photon drag effect – has been observed in a broad range of incidence angles. The angular profile of the electric response nearly mirrored the SPP reflectance profile, with the maximum of the electric signal corresponding to the minimum of the SPP reflectance, Fig. 1b. The sign of the photon drag effect at the *resonance* angle, corresponding to the excitation of SPP, was different from that at *off-resonance* angles, at which the projection of the photon wave-vector onto the plane of the silver film did not match the wave-vector of the SPP. Thus, electrons dragged by resonantly excited SPPs propagated along the projection of the incident photon wavevector onto the film surface, while at off-resonance incidence angles, electrons were dragged in the direction opposite to the photon wavevector.

The magnitude of the electric signal at resonant excitation exceeded that of the off-resonant signal fivefold to tenfold. Both resonant and off-resonant electric signals were nearly linearly proportional to the laser light intensity at small excitation energies and showed some saturation at larger pumping values, Fig. 1d. Despite of relatively small voltages measured, the peak current density in our experiments, calculated taking into account electrical resistance and cross-section of the silver strip, was very high, up to 10 A/mm^2, which is larger than the maximal working current density in insulated copper wires, 6 A/mm^2 [23]. When the film was illuminated from the other cathetus face of the prism, with the reversed direction of the in-plane component of the wavevector, both on-resonance and off-resonance electric signals reversed signs accordingly, inset of Fig. 1c. This, again, corresponded to the drift of electrons along the projection of the photon wavevector at the resonant SPP excitation conditions and against the wavevector's projection at the angles at which SPPs were not resonantly excited.

3. Control of Surface Plasmon Polaritons by External Current

In another set of experiments, a strip of silver film on the prism was illuminated with a cw He-Ne laser (λ=632.8 nm) while rectangular voltage pulses were applied to the film by a pulse generator (~1V, t_{pulse}=1ms), Fig. 2a. The driving voltage caused the change of the reflectance ΔR, which temporal profile followed the shape of the voltage pulse, Fig. 2b. A lack of noticeable delay of ΔR in respect to the control voltage pulse makes thermal-related explanations of the effect unlikely. The dependence of ΔR on the excitation angle θ closely followed the reflectance profile of the SPP $R(\theta)$, although it had a much smaller amplitude and an opposite sign. (When $\Delta R(\theta)$ was multiplied by –60000 and some constant was added, its angular profile closely overlapped that of $R(\theta)$, Fig. 2c.)

4. Discussion of the experimental results

Let us start the discussion by making a comment that the *light pressure* model [10] cannot adequately describe the photoinduced effects observed in our experiments. At the laser power density P = 6 kW/mm^2, incidence angle θ = 30 deg, silver reflectance R = 0.95 and electron relaxation time $\tau = 10^{-14}$ s, the calculated current, J~1.5 μA, is of the opposite sign and nearly one order of magnitude smaller than that experimentally measured at the off-resonance excitation, ~20 μA. It is also nearly two orders of magnitude smaller than the one detected at the SPP resonance angle, 0.1-0.2 mA. We, thus, conclude that the simple light pressure model or the light pressure magnified by an enhanced, up to ten-fold, photon absorption at the SPP resonant excitation (as was suggested in Ref. [15]) cannot be an explanation for the observed effect.

The resemblance of the angular dependences of the photoinduced current, $I(\theta)$, and the reflectance, $R(\theta)$, in Fig. 1b unambiguously suggests that at the resonant condition of the surface

plasmon polariton (SPP) excitation, SPP is the major enabling mechanism of PDE. We infer that the strong photon drag effect in this case is caused by the electron-plasmon coupling previously reported in the literature [17-21]. Then what is the origin of the photon drag effect observed at off-resonance excitation and how one can explain the change of the sign of the photoinduced current as the incidence angle is scanned through the SPP resonance? These questions are addressed in the discussion to follow.

Among the effects experimentally observed in this work, particularly intriguing is the change of the sign of the photoinduced current when the incidence angle is scanned through the SPP resonance angle, Fig. 1b. This angular-dependent change of polarity correlates with the change of distribution of electric field intensity between the front (glass-metal) and rear (metal-air) surfaces of the silver film, Fig. 3. Thus, the field near the rear surface of the film has a sharp maximum at the SPP resonance angle, where it is much stronger than the field at the film's front surface. At the same time, the field near the front surface of the metallic film prevails over that at the rear surface at off-resonance angles, Fig. 3. Note that in Fig. 3, the width of the electric field profile is slightly larger than that of the reflectance profile, in a good agreement with Fig. 1b, in which the width of $I(\theta)$ is slightly larger than the width of $R(\theta)$.

The reversed direction of the current (electrons moving opposite the projection of the photon wavevector) at off-resonant excitation angles is in a qualitative agreement with the photogalvanic model of Refs. [10-12]. Thus, electric field in metal produced by p polarized light, which wave-vector has negative x component and positive z component, drives electrons along line 1-2 in right inset of Fig. 3. Because of a vicinity of diffusely scattering metal surface, electrons driven toward the interface (at point A) have shorter paths (truncated by the scattering at the surface) and shorter displacements along the negative x direction than electrons driven away from the

interface, which have longer displacements along the positive x direction. This creates a net surface current in the positive x direction, opposite to the projection of the photon wavevector onto the metallic surface. The photogalvanic model predicts the angular dependence of the photogalvanic current to be $\propto\sin(2\theta)$ [10]. In the range of the incidence angles studied (between 32^o and 46^o) this function is nearly constant, Fig. 1b. (Note that given short DeBroglie wavelength of free electrons in silver (~5Å), which is much smaller than the surface roughness (≥3 nm), electron scattering at the film surface can always be treated as diffuse.) One can infer that a similar process occurring near the rear surface of the metallic film (at the resonant SPP angle, when the electric field is shifted to the rear) would induce electron current flowing in the opposite direction – *along* the projection of the photon wave-vector.

Alternatively, depending on characteristic roughness of the silver films studied, which can be further magnified by long laser exposures, incident photons can be scattered to SPPs propagating along the projection of the photon wavevector, in the opposite direction, or localized [25-27]. Assuming that the character of the scattering surface favored high spatial frequency components ($k\geq10^5$ cm^{-1}) [25] over low spatial frequency components, SPPs facilitated by scattering (at off-resonance incidence angles) and, correspondingly, electron current in our experiment, predominantly propagated in the direction opposite to the projection of the photon momentum. Note that scattering can result in depolarization of incident light [28], enabling SPP excitation at both s and p polarizations.

Thus, while strong PDE effect observed at the resonant incidence angle is primarily due to the SPP excitation and electron-plasmon coupling [17-21], photocurrents induced at off-resonance angles have contributions from both SPPs excited via surface roughness and electron scattering at the surface. The combined effects of front and rear surfaces of a metallic film enrich

and complicate the underlying physics of the phenomenon. These effects as well as the surface roughness, corresponding correlation lengths, and effects of laser exposure will be carefully studied and published elsewhere. Although other possible enabling mechanisms of PDE, *e.g.* the ones associated with the Doppler effect [9] or the striction forces [16] cannot be excluded, at this point we do not have evidence of their significant roles.

To investigate the nature of the control of SPPs with an external current discussed in Section 3, we modeled the angular profile $\Delta R(\theta)$ expected at the change of real ε' and imaginary ε'' parts of electric permittivity of the silver film or its thickness d. The latter hypothetically could be a result of a (not likely) thermal expansion. The corresponding profiles $\Delta R(\theta)$, calculated at small (sometimes unrealistically small) deviations of ε', ε'' and d from their nominal values, are compared with the experimental result in Figs. 4a-4c. Although the calculated values $\Delta R(\theta)$ are of the same order of magnitude as the experimental ones, they do not fit the experiment qualitatively or quantitatively. (The agreement between the model and the experiment is slightly better in Fig. 4c than in Figs. 4a and 4b. However, it is still not as good as the agreement between $R(\theta)$ and $\Delta R(\theta)$ curves in Fig. 2c.) Larger or smaller values of $\Delta\varepsilon'$, $\Delta\varepsilon''$, and Δd than those used in Figs. 4a, 4b, and 4c, cause an even larger mismatch between the model and the experiment. Therefore, the explanation of the observed phenomenon is beyond simple current-induced changes of the basic film parameters. As the electron-plasmon interaction [17-21] couples SPP with electrons, it is a highly plausible mechanism contributing to the control of SPPs with external currents.

5. Summary

To summarize, we have observed (*i*) SPP-enhanced photon drag effect with a record-high current density (10 A/mm^2), and (*ii*) moderately weak ($<10^{-4}$) control of SPPs with an external current.

Both effects are manifestations of electron-plasmon coupling and enhancement of electron drag by plasmons. The observed phenomena pave the road to a variety of opto-electronic devices and nanocircuitry operating at optical frequencies.

The work was supported by the NSF PREM grant # DMR 0611430, NSF NCN grant # EEC-0228390, AFOSR grant # FA9550-09-1-0456, and subcontract from UTC #10-S567-001502C4. The authors cordially thank Vladimir M. Shalaev for stimulating discussions.

References

1. N. Engheta, Science **317**, 1698 (2007).

2. A. M. Danishevskii *et al*., Sov. Phys. JETP **31**, 292 (1970).

3. A. F. Gibson, M. F. Kimmitt and A. C. Walker, Appl. Phys. Lett. **17**, 75 (1970).

4. A A Serafetinides and M F Kimmitt, J. Phys. D: Appl. Phys. **11**, L97 (1978).

5. A. F. Gibson and S. Montasser, J. Phys. C **8**, 3147 (1975).

6. S. Luryi, Phys. Rev. Lett. **58**, 2263–2266 (1987).

7. A. A. Grinberg and S. Luryi, Phys. Rev. Lett **67**, 156 (1991).

8. V. M. Shalaev, C. Douketis, and M. Moskovits, Phys. Lett. A **169**, 205 (1992).

9. V. M. Shalaev *et al*., Phys. Rev. B **53**, 11388 (1996).

10. V. L. Gurevich, R. Laiho, and A. V. Lashkul, Phys. Rev. Lett. **69**, 180 (1992).

11. V. L. Gurevich, R. Laiho, Phys. Rev. B **48**, 8307(1993).

12. V. L. Gurevich and R. Laiho, Phys. Sol. St. **42**, 1807 (2000).

13. M. L. Stockman, L. N. Pandey, and T. F. George, Phys. Rev. Lett. **65**, 3433 (1990).

14. J. E. Goff and W. L. Schaich, Phys. Rev. B **56**, 15421 (1997).

15. A. Vengurlekar and T. Ishiara, Appl. Phys. Lett. **87**, 091118 (2005).

16. M. Durach, A. Rusina, and M. I. Stockman, Phys. Rev. Lett. **103**, 186801 (2009).

17. M. Wegener and W. Hügel, Advances in Solid State Physics **41**, 89 (2001).

18. M. V. Fischetti, Phys. Rev. B **44**, 5527 (1991).

19. K. Flensberg and B. Y.-K. Hu, Phys. Rev. Lett. **73**, 3572 (1994).

20. P. W. A. McIlroy and M. Pepper, J. Phys. C: Solid State Phys. **18**, L87 (1985).

21. M. V. Bashevoy, F. Jonsson, A. V. Krasavin, N. I. Zheludev, Y. Chen, M. I. Stockman, Nano Letters 6, 1113-1115 (2006).

22. H. Raether, *Surface Plasmons on Smooth and Rough Surfaces and on Gratings*. Springer Tracts in Modern Physics **111**. New York: Springer-Verlag 1988.

23. MWS Wire Industries Specifications, http://www.mwswire.com/

24. P. B. Johnson and R. W. Christy, Phys. Rev. B **6**, 4370-4379 (1972).

25. H. Ogura and Z. L. Wang, Phys. Rev. B **53**, 10358 (1996).

26. S. Bozhevolnyi and F. Pudin, Phys. Rev. Lett. **78**. 2923 (1997).

27. M. A. Noginov *et al*., Phys. Rev. Lett. **101**, 226806 (2008).

28. K. Gåsvik, Optics Comm. **22**, 61 (1977).

Figure captions

Figure 1. Photon drag effect experiment. (a) Experimental setup. (b) SPP reflectance angular profile (red circles) and angular profile of the electric signal (blue diamonds). Solid line in the bottom: function $\propto -\sin(2\theta)$. (c) Electric signal kinetics. Inset: same for excitation of the prism from the other cathetus face. (d) Dependence of resonant (1) and off-resonant (2) electric signals on the excitation energy.

Figure 2. Controlling light with current. (a) Experimental setup. (b) Pulse of electric signal from a pulse generator (red trace on the top) and corresponding pulse in the detected optical signal (blue trace in the bottom) (c) SPP reflectance angular profile (red circles – experiment and solid line – calculation) and corresponding to it angular profile of the electrically induced change of reflectance ΔR (blue squares, multiplied by –60000 and with added constant 0.26).

Figure 3. Left inset: Distribution of the x component of electric field in the Kretschmann geometry at the resonant angle corresponding to excitation of SPP (43.8^o, lower panel) and at the off-resonance angle (46.8^o, upper panel). The 50 nm silver film is sandwiched between glass and air. Main panel: Angular dependence of the x component of electric field in the silver film 5 nm above the silver-air interface (trace 1) and 5 nm below the glass-silver interface (trace 2). Trace 3 represents angular reflectance profile. In calculations: index of refraction of glass n=1.78, real part of electric permittivity of silver ε'=-14.2, imaginary part of the electric permittivity of silver ε''=0.42 [24], wavelength λ=594 nm. Calculations are done with the COMSOL Multiphysics software. Right inset: Diffused scattering of electrons at the metal surface, determining a photogalvanic effect [11].

Figure 4. Profiles $\Delta R(\theta)$ calculated at small deviations of ε' (a), ε'' (b) and d (c) from their nominal values, as shown on the plots, (solid lines) and the experimental profile $\Delta R(\theta)$ (squares).

Figure 1.

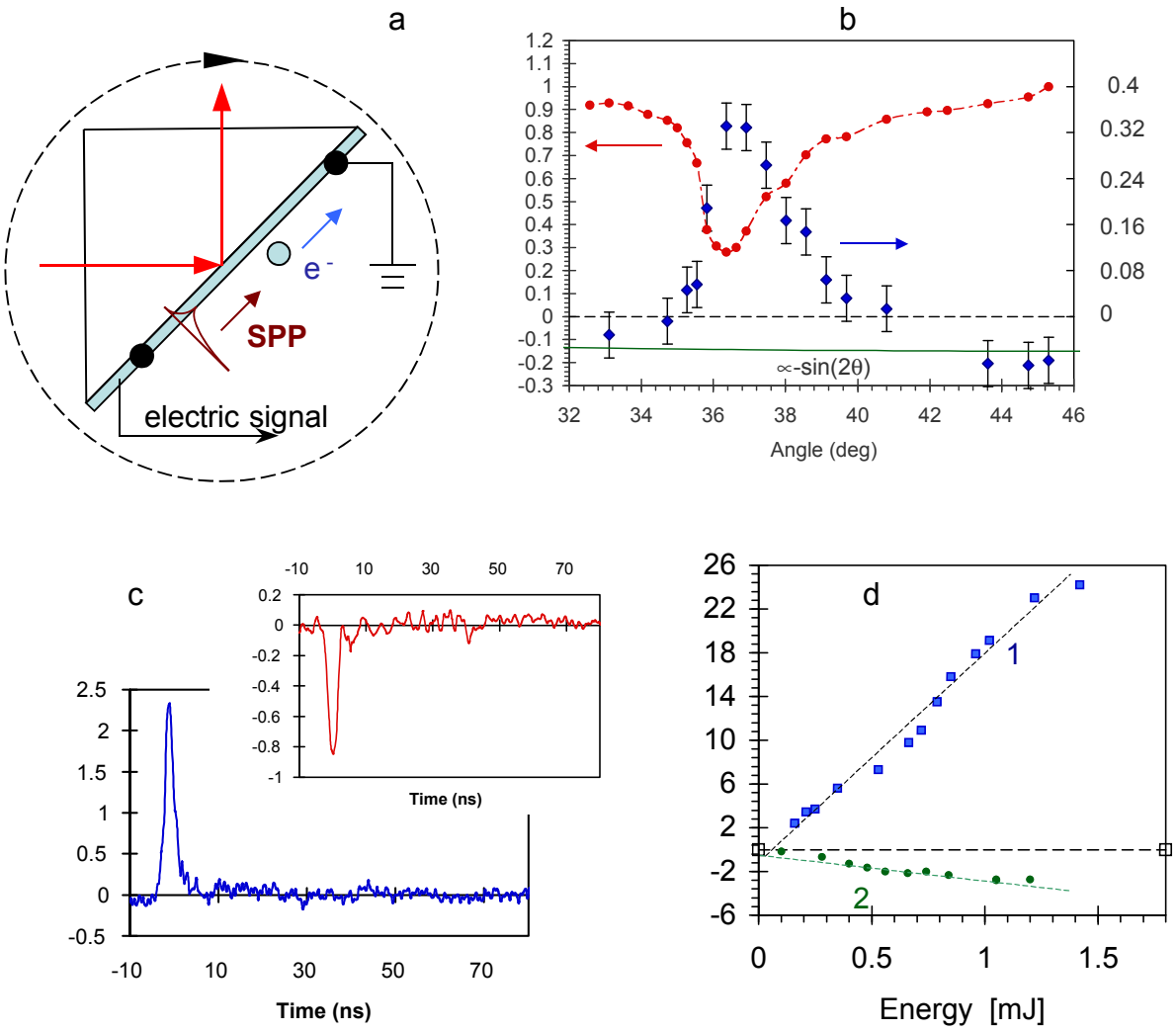

Figure 1. Photon drag effect experiment. (a) Experimental setup. (b) SPP reflectance angular profile (red circles) and angular profile of electric signal (blue diamonds). Solid line in the bottom: function $\propto -\sin(2\theta)$. (c) Electric signal kinetics. Inset: same for excitation of the prism from the other cathetus face. (d) Dependence of resonant (1) and off-resonant (2) electric signals on excitation energy.

Figure 2.

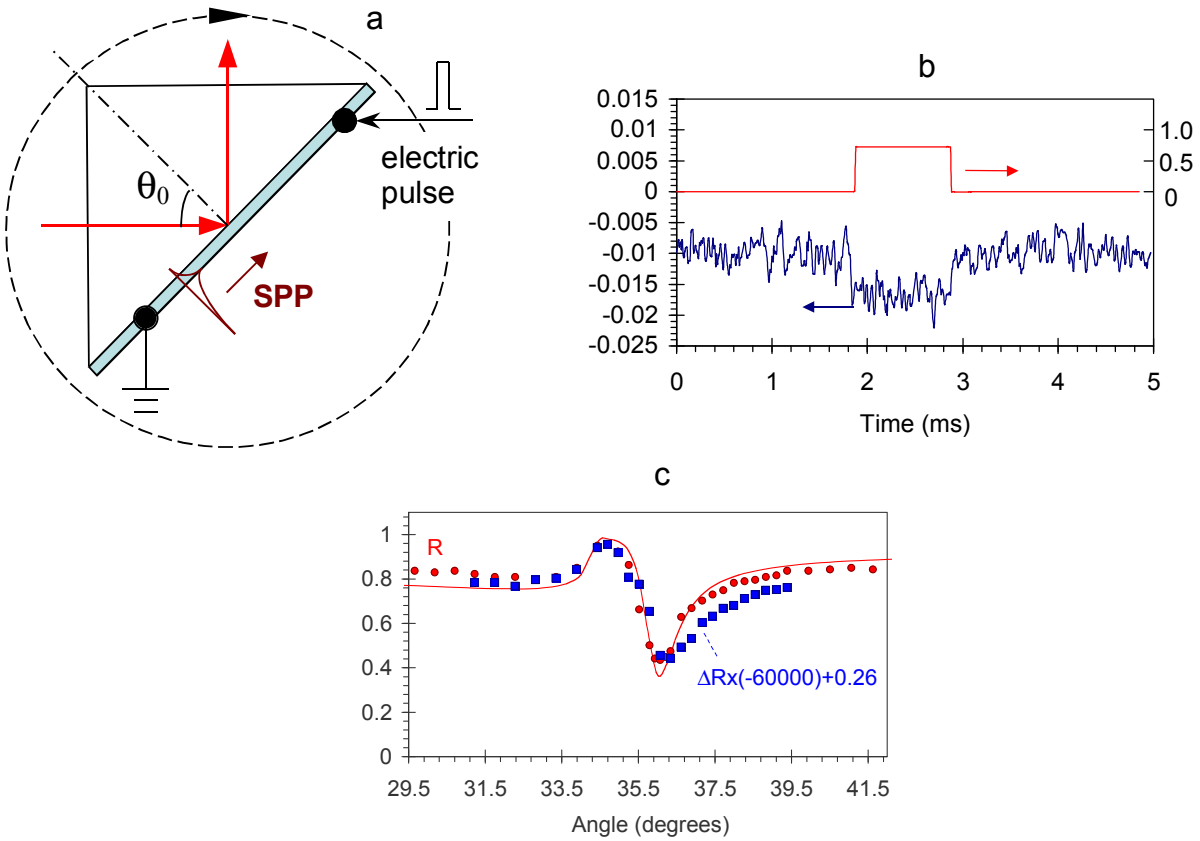

Figure 2. Controlling light with current. (a) Experimental setup. (b) Pulse of electric signal from pulse generator (red trace on the top) and corresponding pulse in the detected optical signal (blue trace in the bottom) (c) SPP reflectance angular profile (red circles – experiment and solid line – calculation) and corresponding to it angular profile of electrically induced change of reflectance ΔR (blue squares, multiplied by –60000 and with added constant).

Figure 3.

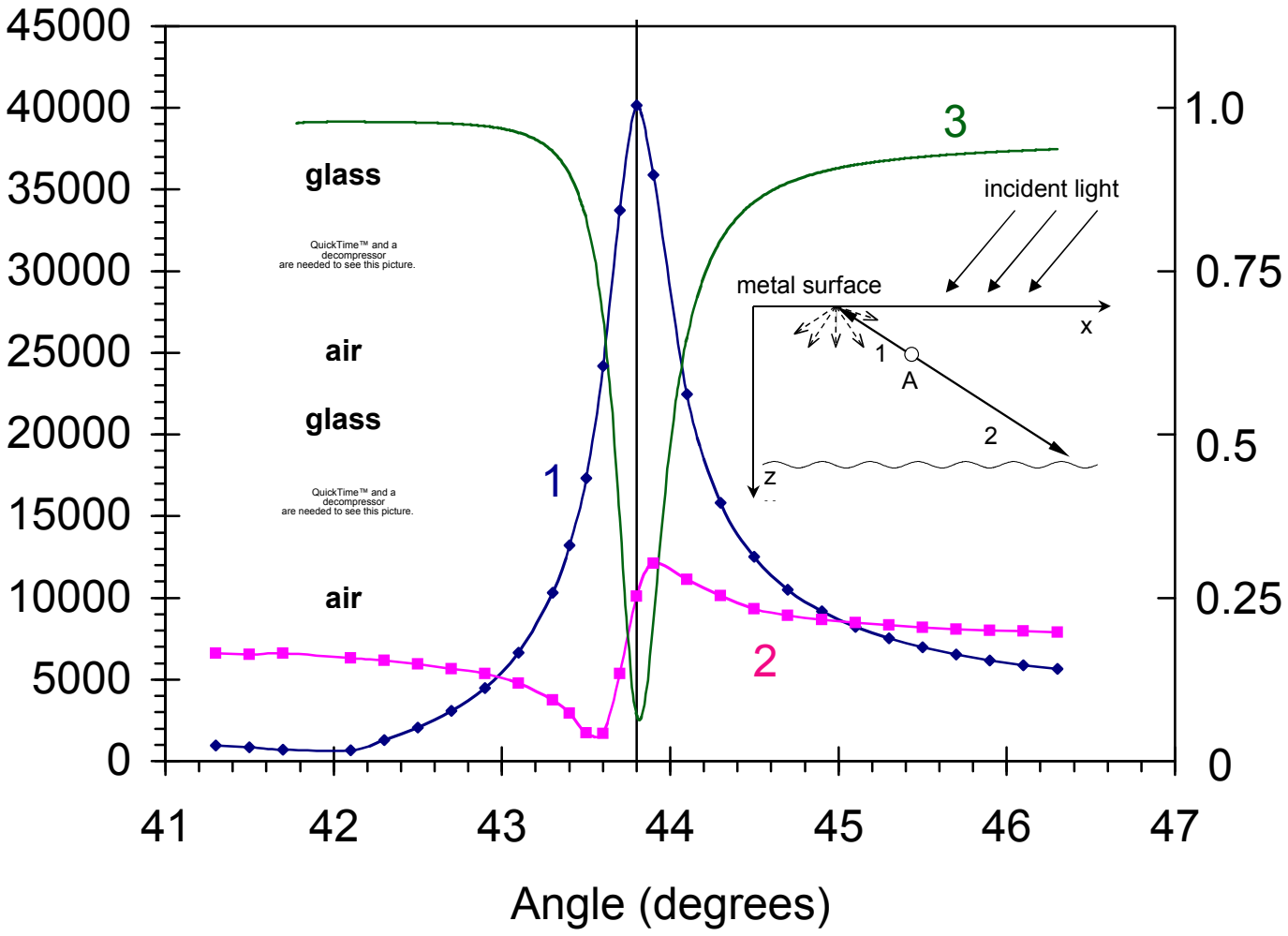

Figure 3. Left inset: Distribution of the x component of electric field in the Kretschmann geometry at the resonant angle corresponding to excitation of SPP (43.8^o, lower panel) and at the off-resonance angle (46.8^o, upper panel). The 50 nm silver film is sandwiched between glass and air. Main panel: Angular dependence of the x component of electric field in the silver film 5 nm above the silver-air interface (trace 1) and 5 nm below the glass-silver interface (trace 2). Trace 3 represents angular reflectance profile. In calculations: index of refraction of glass n=1.78, real part of electric permittivity of silver ε'=-14.2, imaginary part of the electric permittivity of silver ε''=0.42 [24], wavelength λ=594 nm. Calculations are done with the COMSOL Multiphysics software. Right inset: Diffused scattering of electrons at the metal surface determining a photogalvanic effect [11].

Figure 4.

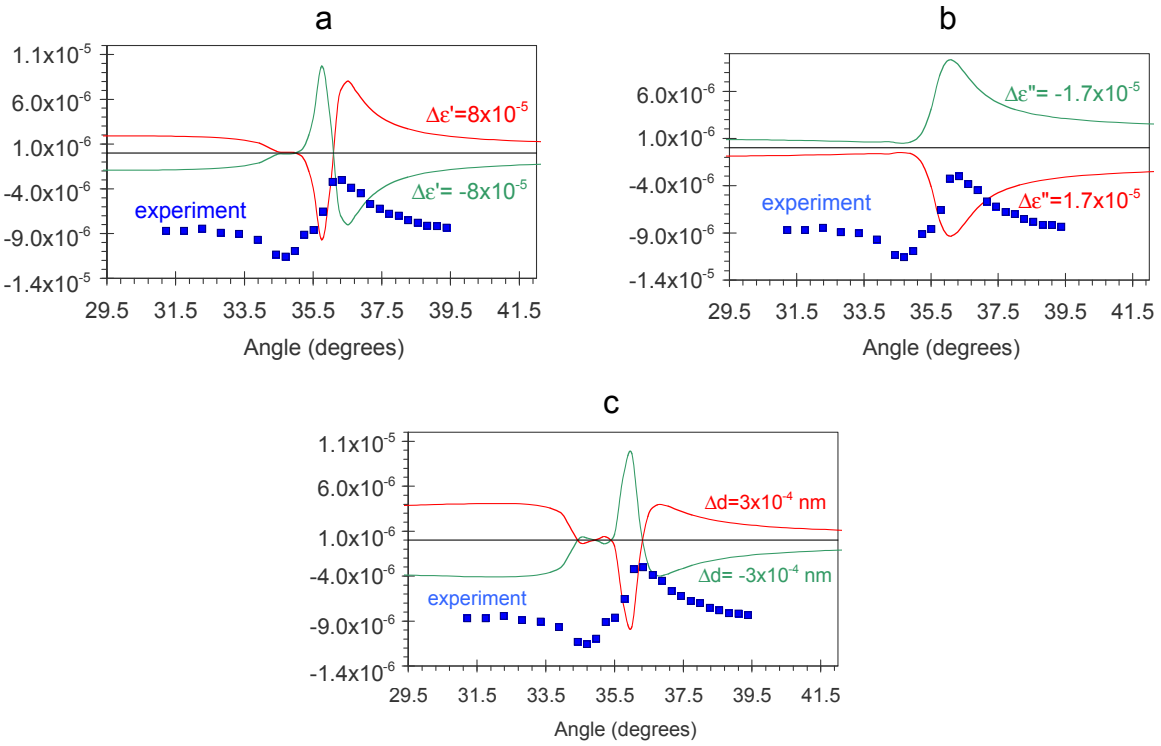

Figure 4. Profiles $\Delta R(\theta)$ calculated at small deviations of ε' (a), ε'' (b) and d (c) from their nominal values as shown on the plots (solid lines) and the experimental profile $\Delta R(\theta)$ (squares).